

OUTWARD PROPAGATION VELOCITY AND ACCELERATION CHARACTERISTICS IN HYDROGEN-AIR DEFLAGRATION

Katsumi, T.¹, Kobayashi, H.², Aida, T.³, Aiba, K.⁴ and Kadowaki, S.⁵

¹ Department of Mechanical Engineering, Nagaoka University of Technology, Kamitomioka 1603-1, Nagaoka, 940-2188, Japan, katsumi@mech.nagaokaut.ac.jp

² Graduate School of Engineering, Nagaoka University of Technology, Kamitomioka 1603-1, Nagaoka, 940-2188, Japan, s113041@stn.nagaokaut.ac.jp

³ Graduate School of Engineering, Nagaoka University of Technology, Kamitomioka 1603-1, Nagaoka, 940-2188, Japan, s123001@stn.nagaokaut.ac.jp

⁴ Graduate School of Engineering, Nagaoka University of Technology, Kamitomioka 1603-1, Nagaoka, 940-2188, Japan, s133001@stn.nagaokaut.ac.jp

⁵ Department of System Safety, Nagaoka University of Technology, Kamitomioka 1603-1, Nagaoka, 940-2188, Japan, kadowaki@mech.nagaokaut.ac.jp

ABSTRACT

Propagation characteristics of hydrogen-air deflagration need to be understood for an accurate risk assessment. Especially, flame propagation velocity is one of the most important factors. Propagation velocity of outwardly propagating flame has been estimated from burning velocity of a flat flame considering influence of thermal expansion at a flame front; however, this conventional method is not enough to estimate an actual propagation velocity because flame propagation is accelerated owing to cellular flame front caused by intrinsic instability in hydrogen-air deflagration. Therefore, it is important to understand the dynamic propagation characteristics of hydrogen-air deflagration. We performed explosion tests in a closed chamber which has 300mm diameter windows and observed flame propagation phenomena by using Schlieren photography. In the explosion experiments, hydrogen-air mixtures were ignited at atmospheric pressure and room temperature and in the range of equivalence ratio from 0.2 to 1.0. Analyzing the obtained Schlieren images, flame radius and flame propagation velocity were measured. As the result, cellular flame fronts formed and flame propagations of hydrogen-air mixture were accelerated at the all equivalence ratios. In the case of equivalent ratio $\phi=0.2$, a flame floated up and could not propagate downward because the influence of buoyancy exceeded a laminar burning velocity. Based upon these propagation characteristics, a favorable estimation method of flame propagation velocity including influence of flame acceleration was proposed. Moreover, the influence of intrinsic instability on propagation characteristics was elucidated.

1.0 INTRODUCTION

Hydrogen is focused on as a favorable alternative fuel because of zero emissions of carbon dioxide and particulates. Meanwhile, hydrogen has also dangerous characteristics, such as wide flammable range and high burning velocity, and has tendency to cause explosions which include both detonation and deflagration. In the future when hydrogen will be used practically and widely, a serious accident has to be avoided. Based upon the concept of system safety, risk assessment is important to reduce and prevent unacceptable risks.[1] For an appropriate risk assessment, it is necessary to estimate accurately hazards of hydrogen. Flame propagation velocity is one of most important factor and needs to be estimated appropriately. In a conventional method, propagation velocity of outward propagating flame was derived from propagation velocity of a flat flame, considering the influence of thermal expansion. Actually, in the case of hydrogen-air deflagration, a cellular flame front forms owing to the intrinsic instability and flame propagation accelerates. With increasing a radius of outwardly propagating flame, the cellular flame front develops and the flame front area becomes larger. Because a flame propagation velocity depends on a flame front area, flame propagation accelerates with increasing a

flame radius. In a huge space, flame propagation keeps on accelerating because cellular flame front develops more.

Previously, the hydrogen-air deflagration has been investigated in a large closed chamber and in the open air by Kwon et al., Okafor et al., and Kim et al.[2-4] However, dynamic characteristics of flame propagation and flame instability was not understood enough to predict propagation phenomena of outwardly propagating flame. In the case of experiment in a closed chamber, large flame cannot be observed because of small window. And, in the case of experiment in the open air, detail structure of flame cannot be clarified because of low-resolution images. In this study, we prepared a high resolution video camera and a closed chamber which has relatively large windows and investigated the propagation characteristics of hydrogen-air deflagration in order to establish a flame propagation model of outwardly propagating flame.

2.0 EXPERIMENT AND ANALYSIS

Explosion experiments were performed in a closed chamber. As shown in Fig.1, the closed chamber has four quartz windows, whose diameters are 300mm, on the side walls. The internal shape is an intersection of three cylinders and inner volume is 73 liters. For ignition, the chamber has two electrodes which are inserted vertically and oppositely. The overall schematic view of the experimental apparatus is illustrated in Fig.2. The flame propagation phenomena were observed by Schlieren photography (Mizojiri SL-350) through the quartz windows and recorded by using a high-speed video camera (Photoron SA-X) which was operated at 10,000fps with 1024×1024 pixel image resolution. Chamber pressure was measured by a capacitive pressure sensor (Kistler 6045A31), and also initial temperature was measured by a thermocouple (T-type). In the experiments, the chamber was vacuumed and filled with air and hydrogen up to 101kPa, considering each partial pressure. After that, hydrogen-air mixture was ignited at the center of the chamber. By a trigger from the ignition controller, the high speed video camera and the data logger for pressure were synchronized.

In order to evaluate influences of equivalence ratio on propagation characteristics, mixture ratio of hydrogen and air was changed in the range of equivalence ratio, ϕ , from 0.2 to 1.0. Initial pressure, P_0 , and initial temperature, T_0 , of the mixtures were kept at constant, 298K and 101kPa, respectively.

Furthermore, we analyzed images of the obtained Schlieren video frame-by-frame. First, a mean flame radius, r , was obtained from area occupied by a flame shadow in a Schlieren image. Second, flame propagation velocity, S_b , was derived by differentiating the flame radius with respect to time. Based upon these values, correlation between flame radius and flame acceleration was evaluated.

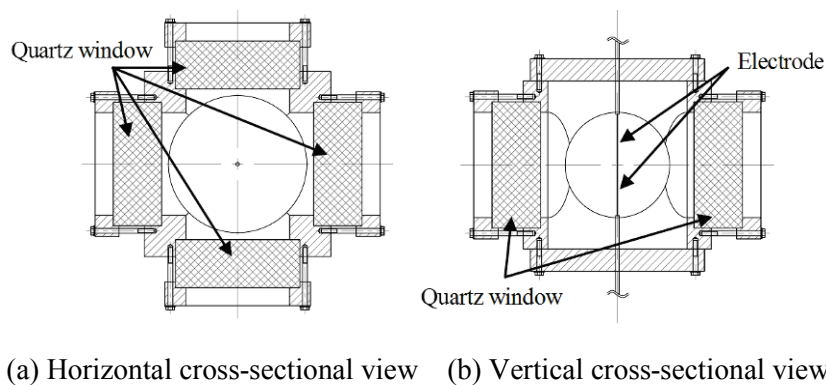


Figure 1. Schematic view of closed chamber

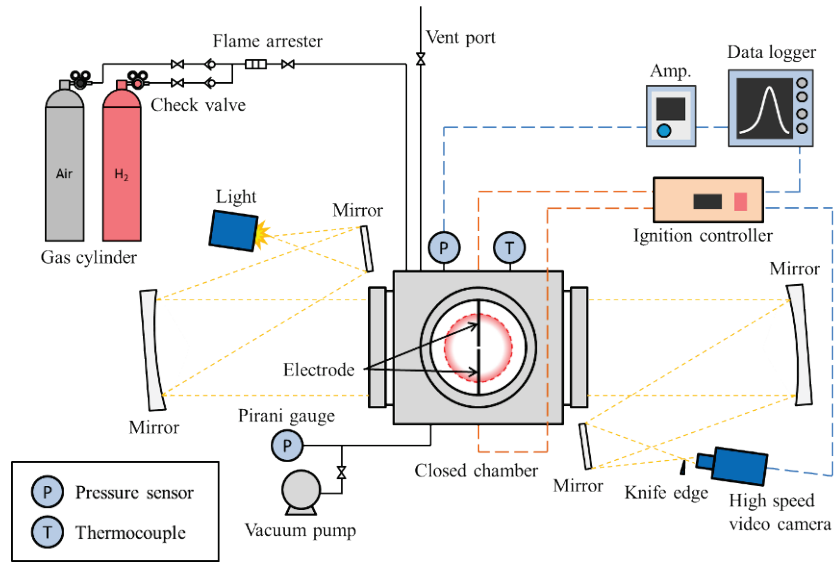


Figure 2. Schematic view of experimental apparatus

3.0 RESULTS

Figure 3~5 show the Schlieren images of outwardly propagating flames in the cases of $\phi=0.9$, 0.6 and 0.3. In each equivalence ratio, flame shapes observed at approximately 2.0cm, 4.0cm, 8.0cm and 12.0cm in radius are presented. In more than $\phi=0.3$, cellular flame fronts formed and wrinkles at the flame front increased with the increasing of flame radius. Comparing between different equivalence ratios at same diameter, a flame front in the case of lower equivalence ratio has more wrinkles and larger concave/convex than that of higher equivalence ratio. This result clarifies that the cellular flame front develops more at lower equivalence ratio.

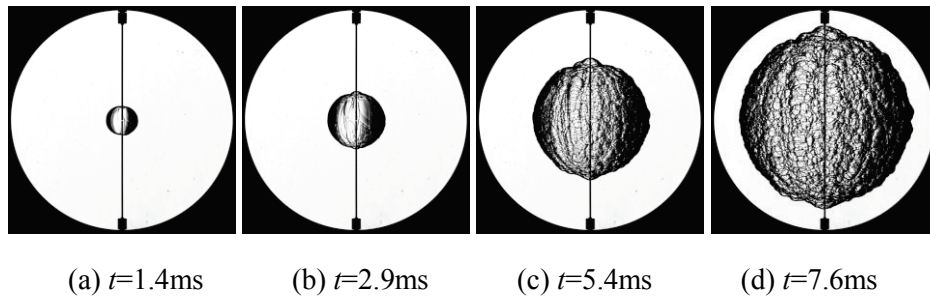


Figure 3. Schlieren photograph ($\phi=0.9$, $T_0=298\text{K}$, $P_0=101.3\text{kPa}$)

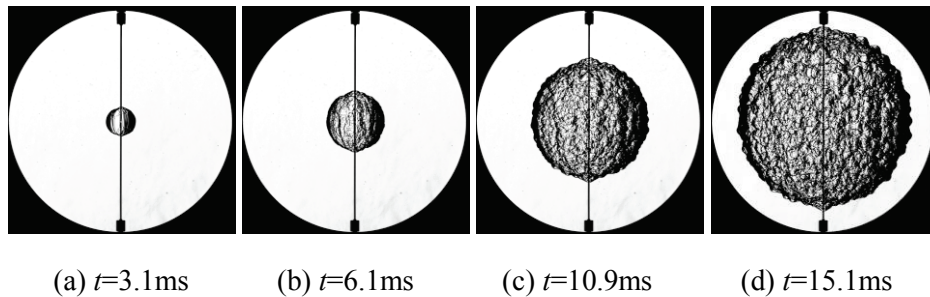


Figure 4. Schlieren photograph ($\phi=0.6$, $T_0=298\text{K}$, $P_0=101.3\text{kPa}$)

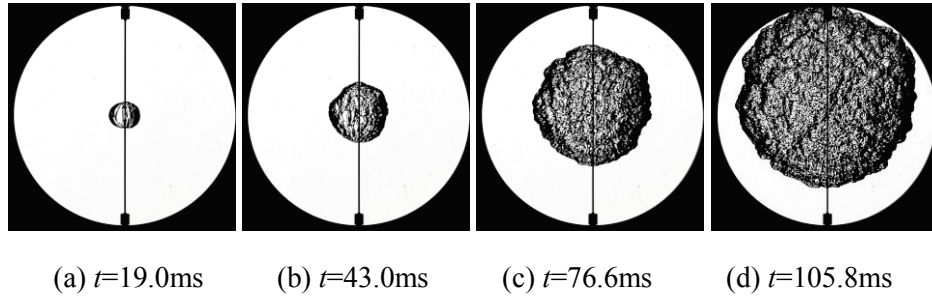


Figure 5. Schlieren photograph ($\varphi=0.3$, $T_0=298\text{K}$, $P_0=101.3\text{kPa}$)

Figure 6 shows the Schlieren images obtained at $t=100\text{ms}$, 200ms , 300ms and 400ms in the case of $\varphi=0.2$. As shown in Fig.6, a flame floated up and did not propagate downward because the influence of buoyancy exceeds a laminar burning velocity.

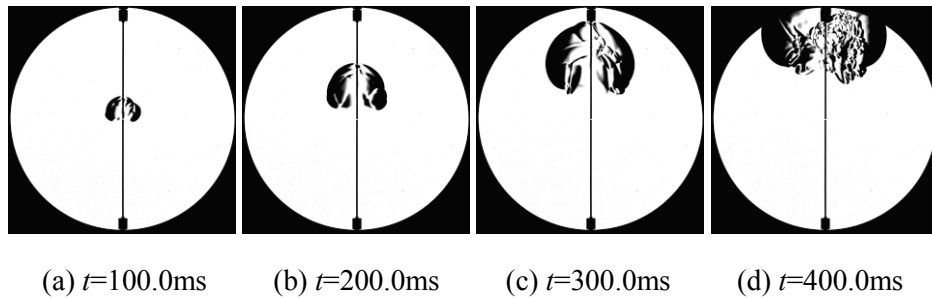


Figure 6. Schlieren photograph ($\varphi=0.2$, $T_0=298\text{K}$, $P_0=101.3\text{kPa}$)

Analysing the Schlieren videos, we succeeded in obtaining profiles of flame propagation velocity, S_b . Figure 7 shows the dependency of flame propagation velocity on flame radius, r , in the range of equivalent ratio, from 1.0 to 0.3. In the case of $\varphi=0.2$, the flame radiuses could not be measured because of flame floating up. Flame propagation velocity in the case of higher equivalence ratio is higher than that of lower equivalence ratio owing to characteristics of laminar burning velocity. Also, flame propagation velocities increase with increasing the flame radius in these equivalence ratios.

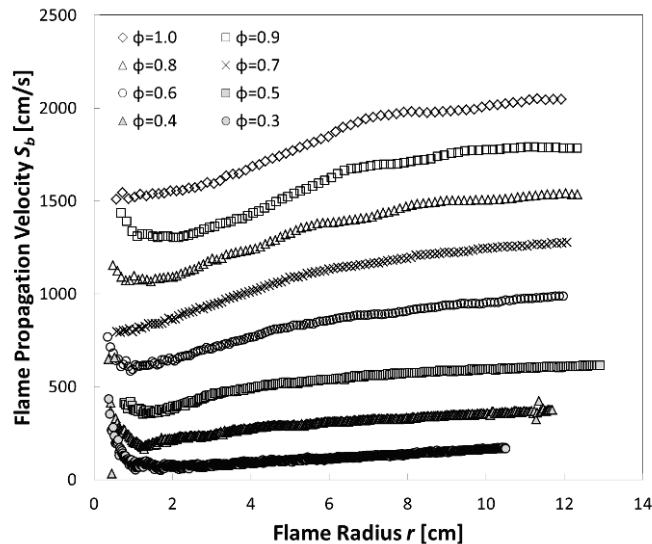


Figure 7. Dependency of flame propagation velocity on flame radius

In addition, inside pressure profiles of the chamber as a function of flame radius are plotted in Fig.8. The pressures in all equivalence ratios increased by approximately 10% of the initial pressures when the flame radiuses reached the measurable limit, $r \approx 12$ cm.

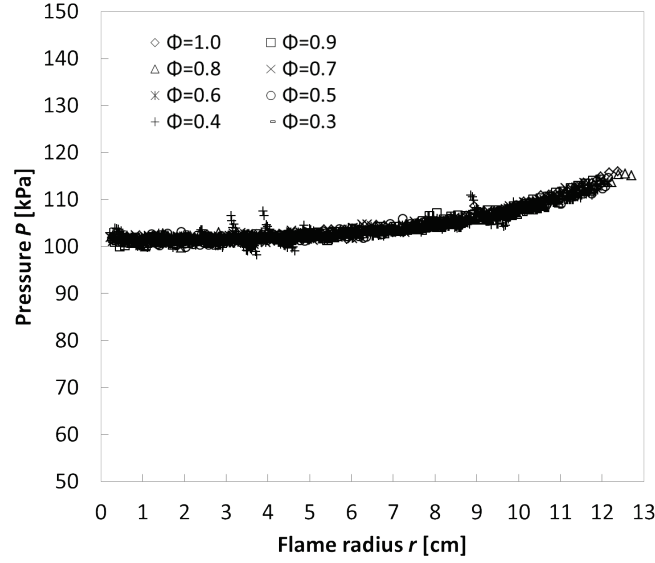


Figure 8. Inside pressure profiles of the chamber

4.0 DUSCUSSION

4.1 Propagation Velocity of Flat Flame

Propagation velocities of flat flames, S_{b0} , were estimated based upon the experimental data. In the case of small radius, flame propagation velocity is not affected by cellular flame because flame front is smooth at less flame radius than a certain critical radius, r_0 . However, flame stretch influences on a burning velocity. Burning velocity correlated linearly with flame stretch rate as shown in Eq.1. Here, S_u is burning velocity, S_{u0} is burning velocity of unstretched flat flame, κ is flame stretch rate and Ma is Markstein number.

$$S_u - S_{u0} = \kappa Ma, \quad (1)$$

where the flame stretch rate, κ , is defined as

$$\kappa = 2S_u/r, \quad (2)$$

In addition, in the range of flame radius where a cellular flame does not appear, flame propagation velocity, S_b , can be derived from S_u considering the influence of thermal expansion at a flame front, as shown in Eq.3. Here, ρ_b is density of burnt gas and ρ_u is density of unburnt gas.

$$S_b = S_u(\rho_b/\rho_u), \quad (3)$$

Thus, correlation between S_b and $2S_b/r$ can be expressed as Eq.4.

$$S_b = Ma(\rho_u/\rho_b) \cdot 2S_b/r + S_{b0}, \quad (4)$$

Flame propagation velocity, S_b , can be fitted by Eq.4 in the range of large stretch rate where flame propagation does not accelerate. Subsequently, S_{b0} can be obtained from the y-intercepts of the fitted curves. Obtained propagation velocities of flat flames, S_{b0} , are summarized in Fig.9. The propagation

velocities of flat flame which were obtained from our experimental data show good agreement with the data by other researchers.[5-7]

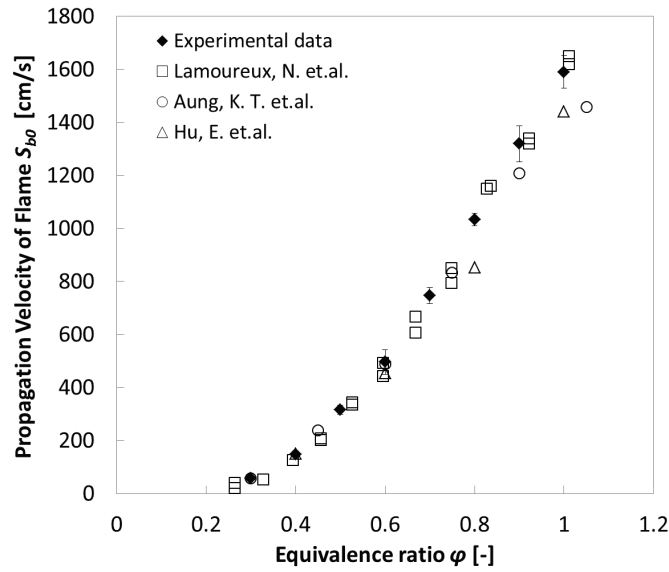


Figure 9. Propagation velocity of flat flame [5-7]

4.2 Flame Acceleration

In the range of less stretch rate than that at an onset of flame acceleration, S_b increases and deviates from the fitted curve which is expressed as Eq.4, because influence of cellular flame front caused by intrinsic instability becomes stronger than influence of flame stretch. In this paper, onset flame radius of flame acceleration is defined as the critical flame radius, r_0 . The critical flame radiuses, r_0 , in each equivalence ratio are summarized in Fig.10. As an equivalence ratio decreases, the critical flame radius becomes small at a higher equivalence ratio than 0.7, and increases at a lower equivalence ratio than 0.6. This fact could indicate that thermal-diffusive instability becomes stronger as an equivalence ratio decreases, while thermal-diffusive instability is suppressed at a lower equivalence ratio than 0.6 because the flame thickness increases as the equivalence ratio decreases.

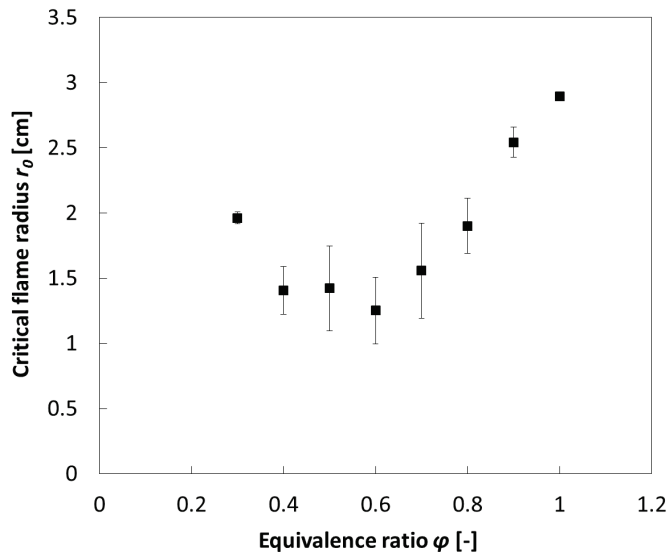


Figure 10. Dependency of critical flame radius on equivalence ratio

Moreover, in order to understand the characteristics of flame acceleration, the dependencies of the flame propagation velocity on flame radius were regressed by a curve. Kadowaki et al expressed a growth rate of disturbance and succeeded in numerical calculation of a cellular flame characteristics using logarithm of characteristic length.[8] Based upon their study, we employed logarithm of a flame radius, $\ln(r^*)$, as a characteristic length and propose Eq.5 for the curve regression.

$$S_b = \alpha \ln(r^*) + \beta, \quad (5)$$

where non-dimensional flame radius, r^* , and the intercept, β , are defined as

$$r^* = r/r_0, \quad (6)$$

$$\beta = S_{b0}, \quad (7)$$

In the ranges of larger flame radius than r_0 at each equivalence ratio, proportionality constants, α , can be obtained based upon the correlation between $\ln(r^*)$ and S_b . Furthermore, Eq.5 is transformed to Eq.8 in order to clarify the effect of flame radius on flame acceleration. In Eq.8, α/β which means the dependency coefficient of flame acceleration on flame radius is summarized at each equivalence ratio in Fig.11.

$$\frac{S_b - S_{b0}}{S_{b0}} = \frac{\alpha}{\beta} \ln(r^*), \quad (8)$$

As shown in Fig.11, α/β increases with decreasing of equivalence ratio. This fact indicates that the flame propagation accelerated more at low equivalence ratio because cellular flame developed more owing to diffusive-thermal instability. The correlation between the equivalence ratio and the growth of cellular flame corresponds to the result of observation.

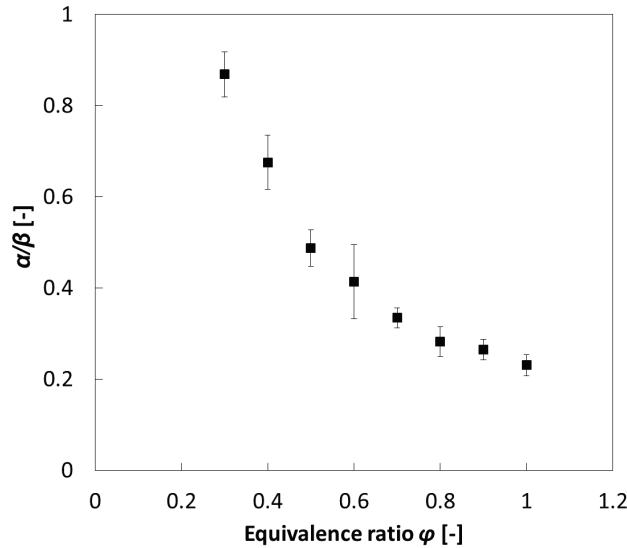


Figure 11. Dependent coefficient of flame acceleration on flame radius, α/β

5.0 CONCLUSION

Explosion experiments of hydrogen-air mixture were performed in the range of the equivalence ratio, from 1.0 to 0.2, by using the closed vessel which has 300mm diameter windows. The propagation phenomena were observed by Schlieren photography. The cellular flame fronts developed with

increasing of flame radius and with decreasing of equivalent ratio. In the case of $\varphi=0.2$, flame floated up owing to influence of buoyancy. Analyzing the Schlieren images, the flame propagation velocities were measured in the case of $\varphi=1.0\sim 0.3$. The flame propagation velocity increased with increasing of flame radius. Based upon the instability study, the dependencies of the flame propagation velocity on flame radius were regressed well by using a logarithm of non-dimensional flame radius. It was found that the dependent coefficient of flame acceleration on flame radius, α/β , becomes higher at lower equivalence ratio. These facts indicate that outward propagation of hydrogen-air deflagration accelerates more at low equivalence ratio because cellular flame develops more owing to diffusive-thermal instability. Conclusively, favorable flame propagation model, Eq.5, and its coefficients, α and β , and critical flame radius, r_0 , were obtained successfully based upon the experimental data. These results can apply to an estimation of flame propagation characteristics and should be useful for an accurate risk assessment.

ACKNOWLEDGEMENTS

The results of this study are performed on the re-entrustment from the LWR hydrogen safety program of the Japan Atomic Energy Agency, which is funded by the Ministry of Economy, Trade and Industry.

REFERENCES

1. JIS B 9700 (ISO 12100:2010) Safety of machinery - General principles for design - Risk assessment and risk reduction, 2013.
2. Kwon, O.C., Rozenchan G., and Law, C.K., Cellular Instabilities and Self-Acceleration of Outwardly Propagating Spherical Flames, *Proceedings of the Combustion Institute*, Vol. 29, Issue 2, 2002, pp. 1775-1783.
3. Okafor, E.C., Hayakawa, A., Nagano, Y., Kitagawa, T., Effects of hydrogen concentration on premixed laminar flames of hydrogen-methane-air, *International Journal of Hydrogen Energy*, Vol. 39, 2014, pp. 2409-2417.
4. Kim, W.K., Mogi, T., Kuwana, K., Dobashi, R., Self-similar propagation of expanding spherical flames in large scale gas explosions, *Proceedings of the Combustion Institute*, Vol. 35, 2015, pp. 2051-2058.
5. Lamoureux, N., Chaumeix, N., Paillard, C.E., Laminar flame velocity determination for H₂-air-He-CO₂ mixtures using the spherical bomb method, *Experimental Thermal and Fluid Science*, Vol. 27, 2003, pp. 385-393.
6. Aung, K.T., Hassan, M.I., Faeth, G.M., Flame stretch interactions of laminar premixed hydrogen/air flames at normal temperature and pressure, *Combustion and Flame*, Vol. 109, 1997, pp. 1-24.
7. Hu, E., Huang, Z., He, J., Miao, H., Experimental and numerical study on laminar burning velocities and flame instabilities of hydrogen-air mixtures at elevated pressures and temperatures, *Hydrogen Energy*, Vol. 34, 2009, pp. 8741-8755.
8. Kadowaki, S., Hasegawa, T., Numerical simulation of dynamics of premixed flames: flame instability and vortex-flame interaction, *Progress in Energy and Combustion Science*, Vol. 31, 2005, pp 193-241.